Published OnlineFirst August 31, 2012; DOI: 10.1158/0008-5472.CAN-12-2026

GF-15, a Novel Inhibitor of Centrosomal Clustering, Suppresses Tumor Cell Growth *In Vitro* and *In Vivo*

Marc S. Raab[1,4,6], Iris Breitkreutz[3,6], Simon Anderhub[2], Mads H. Rønnest[8,9], Blanka Leber[2], Thomas O. Larsen[9], Ludmila Weiz[2,4], Gleb Konotop[4], Patrick J. Hayden[6], Klaus Podar[3,6], Johannes Fruehauf[7], Felix Nissen[5], Walter Mier[5], Uwe Haberkorn[5], Anthony D. Ho[1], Hartmut Goldschmidt[1,3], Kenneth C. Anderson[6], Mads H. Clausen[8], and Alwin Krämer[1,2]

Abstract

In contrast to normal cells, malignant cells are frequently aneuploid and contain multiple centrosomes. To allow for bipolar mitotic division, supernumerary centrosomes are clustered into two functional spindle poles in many cancer cells. Recently, we have shown that griseofulvin forces tumor cells with supernumerary centrosomes to undergo multipolar mitoses resulting in apoptotic cell death. Here, we describe the characterization of the novel small molecule GF-15, a derivative of griseofulvin, as a potent inhibitor of centrosomal clustering in malignant cells. At concentrations where GF-15 had no significant impact on tubulin polymerization, spindle tension was markedly reduced in mitotic cells upon exposure to GF-15. Moreover, isogenic cells with conditional centrosome amplification were more sensitive to GF-15 than parental controls. In a wide array of tumor cell lines, mean inhibitory concentrations (IC_{50}) for proliferation and survival were in the range of 1 to 5 μmol/L and were associated with apoptotic cell death. Importantly, treatment of mouse xenograft models of human colon cancer and multiple myeloma resulted in tumor growth inhibition and significantly prolonged survival. These results show the *in vitro* and *in vivo* antitumor efficacy of a prototype small molecule inhibitor of centrosomal clustering and strongly support the further evaluation of this new class of molecules. *Cancer Res; 72(20); 5374–85. ©2012 AACR.*

Introduction

Centrosomes are small cytoplasmic organelles, which consist of a pair of centrioles embedded in pericentriolar material and act as microtubule-organizing centers. During mitosis, centrosomes function as spindle poles, directing the formation of bipolar spindles, a process essential for accurate chromosomal segregation (1, 2). Centrosomes duplicate precisely once per cell cycle to assure spindle bipolarity, with each daughter cell receiving one centrosome upon cytokinesis. Centrosome amplification is frequent in both solid tumors and hematologic malignancies, and is linked to tumorigenesis and aneuploidy (3–10). The extent of centrosomal aberrations correlates with the degree of chromosomal instability and malignant behavior in tumor cell lines, mouse tumor models, and human tumors (6, 9–12).

In mitosis, supernumerary centrosomes can lead to the formation of multipolar spindles, which is a hallmark of many tumor types (8). Multipolar cell division, however, is antagonistic to cell viability (13, 14). Most progeny derived from a multipolar mitosis will undergo apoptosis. To circumvent this problem, many cancer cells seem to have mechanisms that suppress multipolar division, the best studied being clustering of supernumerary centrosomes into 2 spindle poles enabling bipolar division (8, 13–20). Bipolar spindle formation via centrosomal clustering is associated with an increased frequency of lagging chromosomes during anaphase, thereby explaining the link between supernumerary centrosomes and chromosomal instability (14, 15).

The mechanisms of centrosomal clustering in tumor cells are incompletely understood. Recent genome-wide RNAi screens in cells containing supernumerary centrosomes suggest the involvement of the spindle assembly checkpoint and spindle tension as controlled by the cortical actin cytoskeleton, cell adhesion molecules as well as centrosome and kinetochore components in this process (19, 20).

Supernumerary centrosomes are almost exclusively found in a wide variety of neoplastic disorders but rarely in

Authors' Affiliations: [1]Department of Internal Medicine V, [2]Clinical Cooperation Unit Molecular Hematology/Oncology, German Cancer Research Center and Department of Internal Medicine V; [3]National Center for Tumor Diseases, University of Heidelberg; [4]Max-Eder Group Experimental Therapies for Hematologic Malignancies, German Cancer Research Center (DKFZ); [5]Department of Nuclear Medicine, University Hospital Heidelberg, Heidelberg, Germany; [6]Department of Medical Oncology, Dana-Farber Cancer Institute; [7]Beth Israel Deaconess Medical Center, Harvard Medical School, Boston, Massachusetts; [8]Center for Nanomedicine and Theranostics & Department of Chemistry; and [9]Center for Microbial Biotechnology, Department of Systems Biology, Technical University of Denmark, Kgs. Lyngby, Denmark

Note: Supplementary data for this article are available at Cancer Research Online (http://cancerres.aacrjournals.org/).

M.S. Raab and I. Breitkreutz contributed equally to this work.

Corresponding Author: Alwin Krämer, Clinical Cooperation Unit Molecular Hematology/Oncology, German Cancer Research Center and Department of Internal Medicine V, University of Heidelberg, Im Neuenheimer Feld 581, 69120 Heidelberg, Germany. Phone: 49-6221-42-1440; Fax: 49-6221-42-1444; E-mail: a.kraemer@dkfz.de

doi: 10.1158/0008-5472.CAN-12-2026

Published OnlineFirst August 31, 2012; DOI: 10.1158/0008-5472.CAN-12-2026

nontransformed cells. Therefore, inhibition of centrosomal clustering with consequential induction of multipolar spindles and subsequent cell death would specifically target tumor cells with no effect on normal cells with regular centrosome content (8, 17). Using a phenotype-based screening strategy, we have recently found that griseofulvin induces spindle multipolarity, mitotic arrest, and subsequent cell death in multiple tumor cell lines but not in diploid fibroblasts and keratinocytes with normal centrosome content (13). Chemical optimization of griseofulvin led to the development of compounds with significantly increased activity and mean inhibitory concentrations (IC_{50}) of proliferation and survival in the lower micromolar range when applied to the human squamous cell carcinoma cell line SCC114, which had been used for the initial screening (21).

Here, we present evidence that the exposure of tumor cells to the griseofulvin derivative GF-15 leads to reduced spindle tension, spindle multipolarity, and the inhibition of centrosomal clustering, culminating in the induction of apoptosis *in vitro* and *in vivo*.

Materials and Methods

Materials

(2*S*,6′*R*)-(7-Chloro-4,6-dimethoxy-benzofuran-3-on)-2-spiro-1′-(2′-benzyloxy-6′-methylcyclohex-2′-en-4′-one) (2′-benzyloxy-2′-demethoxygriseofulvin; GF-15) was synthesized following the procedures described recently (21). Caspase-8, caspase-9, γ-tubulin, BubR1, and PARP antibodies were purchased from Santa Cruz Biotechnology. The centrin antibody was kindly provided by J. Salisbury (Rochester).

Cell culture

All human multiple myeloma (MM) cell lines (RPMI-8226, OPM-2, NCI-H929, OPM-1, KMS-12BM, KMS-12PE, KMS-11, KMS-18, U-266, MM1.S, LR5, Dox40, MM1.R) and primary patient MM cells were cultured in RPMI 1640 medium supplemented with 10% heat-inactivated FBS (Harlan), 100 U/mL penicillin, 10 μg/mL streptomycin, and 2 mmol/L L-glutamine (Cellgro). Leukemia lines used were HEL, MOLM14, and Ku812 and cultured as described above. Solid tumor cell lines comprised HeLa (cervical carcinoma), HT29, HCT116, SW480 (colorectal carcinoma), PANC1, PACA1 (pancreatic carcinoma), and LN229 (glioblastoma). HS4, KM105, KM104 (bone marrow stromal cells, BMSC), THLE3 (liver cells), peripheral blood mononuclear cells (PBMC), and primary BMSCs served as nonmalignant controls. All solid tumor cell lines and nonmalignant controls were grown in Dulbecco's Modified Eagle's Medium supplemented with 10% heat-inactivated FBS (Harlan), 100 U/mL penicillin, 10 μg/mL streptomycin, and 2 mmol/L L-glutamine (Cellgro). All cell lines are regularly authenticated by fingerprinting before backup freezing and are kept less than 4 months in culture.

Isolation of patient tumor cells

Patients provided informed consent in accordance with the Declaration of Helsinki. Following approval by the Institutional Review Board of the University of Heidelberg, MM patient cells (96% $CD38^+$ $CD45RA^-$) were obtained as described (22).

Cell lysis and immunoblotting

Cell lysis and Western blot analysis were conducted as described previously (22).

Evaluation of cell viability

Cell viability was examined using the MTT (Sigma Chemical) colorimetric assay, as previously described (23). Briefly, cells were plated in 96-well microtitre plates at a density of $2–3 \times 10^4$ cells per well, and each plate was incubated for 24 and/or 48 hours, with MTT added to each well for at least 4 hours. The absorbance of each well was measured at 570/630 nm using a spectrophotometer (Molecular Devices). Each condition was analyzed in at least 3 replicates, and the results are presented as the mean ± SD of replicates of a representative experiment that was repeated at least 3 times.

DNA synthesis and cell proliferation assay

Cell proliferation was assessed by measuring [^{3}H]-thymidine uptake, as described in prior studies (22).

Measurement of caspase-3/7 activation

Caspase-3/7 activation was analyzed using the Apoptosis Detection Kit from Promega according to the recommendations of the manufacturer.

Flow cytometry

Cell-cycle analysis by flow cytometry was conducted as previously described (13).

Immunofluorescence

Immunofluorescence staining was conducted as described (24). The following fluorochrome-conjugated secondary antibodies were used: anti-rabbit Alexa 488 (Molecular Probes) and anti-mouse Cy3 (Jackson ImmunoResearch Laboratories). Immunostained cells were examined using a Zeiss Axiovert 200 M fluorescence microscope. Images were processed with Photoshop software (Adobe).

Tubulin polymerization assay

The effect of GF-15 on tubulin polymerization was assessed using the tubulin polymerization assay kit (Cytoskeleton) according to the manufacturer's recommendation.

Xenograft mouse models

To determine the *in vivo* activity of GF-15, beige-nude Xid mice were inoculated s.c. in the right flank with 3×10^6 OPM2 or HT29 cells in 100 mL RPMI 1640 medium, together with 100 mL matrigel (Becton Dickinson Biosciences). When a tumor was measurable, mice were assigned to a GF-15 treatment group or the control group. GF-15 was dissolved in 100% dimethyl sulfoxide (DMSO) and given daily 5 times a week by intraperitoneal injection for indicated periods. The control group received the carrier alone at the same schedule and route of administration. Tumor burden was measured every alternate day using a calliper [calculated volume $= 4\pi/3 \times (\text{width}/2)^2 \times (\text{length}/2)$]. Animals were sacrificed when their tumors reached 2 cm in diameter, became exulcerated, or when the mice were moribund. Survival was evaluated from the first

Published OnlineFirst August 31, 2012; DOI: 10.1158/0008-5472.CAN-12-2026

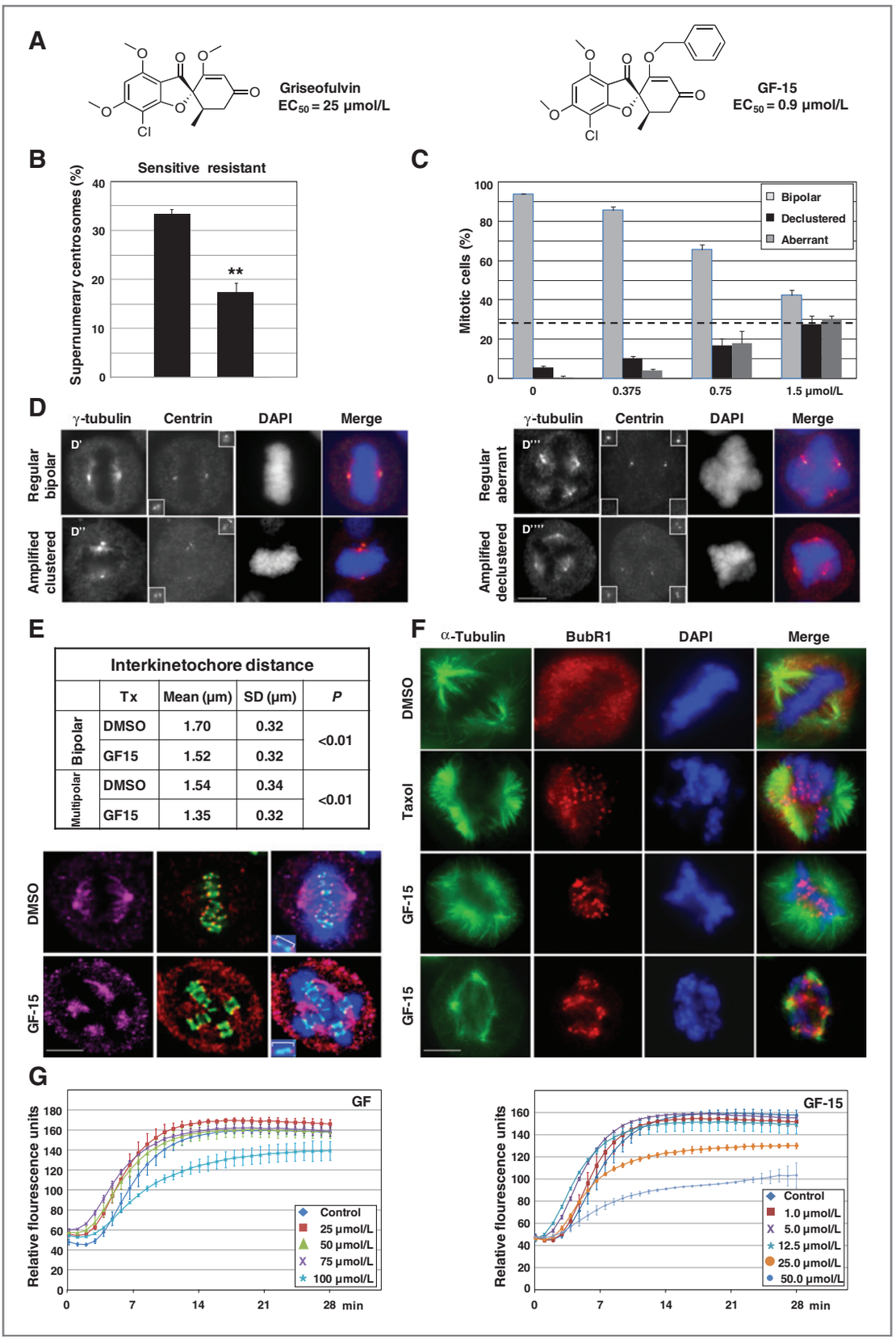

Published OnlineFirst August 31, 2012; DOI: 10.1158/0008-5472.CAN-12-2026

day of treatment until death. All animal studies were approved by the Dana-Farber Animal Care and Use Committee.

Preparation of the radiolabeled GF-15 analogue

[^{125}I/^{131}I]-(2*S*,6′*R*)-(7-Chloro-4,6-dimethoxy-benzofuran-3-one)-2-spiro-1′-(2′-(4-iodo-benzyloxy)-6′-methyl-cyclohex-2′-ene-4′-one) was prepared by thallation-iodination with ^{125}I-iodide or ^{131}I-iodide (Perkin Elmer) of (2*S*,6′*R*)-(7-chloro-4,6-dimethoxy-benzofuran-3-one)-2-spiro-1′-(6′-methyl-2′-(4-trimethylsilylbenzyloxy)-cyclohex-2′-ene-4′-one), which was in turn synthesized from *p*-trimethylsilylbenzyl alcohol (25) using a known method (21). The radiolabeled analogue was compared with a sample of (2*S*,6′*R*)-(7-chloro-4,6-dimethoxy-benzofuran-3-one)-2-spiro-1′-(2′-(4-iodobenzyloxy)-6′-methyl-cyclohex-2′-ene-4′-one) prepared from *p*-iodobenzyl alcohol (22) and found to be identical by high-performance liquid chromatography-mass spectrometry (HPLC-MS) analysis.

Scintigraphic *in vivo* imaging

For imaging studies, 200 μL of a solution of the ^{125}I-labeled GF-15 analogue (5 MBq/mouse) was injected into the tail vein of 6-week-old female NMRI mice. Scintigraphic images were taken using a gamma camera (Biospace). The accumulation of the radioactive tracer was monitored by static planar images at 5 minutes, 15 minutes, 30 minutes, 1 hour, 2 hours, 4 hours, 6 hours, and 24 hours after injection.

Biodistribution studies

^{131}I-labeled GF-15 analogue (1 MBq/mouse) was injected via the tail vein of 6-week-old female NMRI mice. At the time points specified, the animals were sacrificed, weighed, and dissected. Organs or tissues were blotted dry and weighed. The radioactivity was measured in a γ-counter along with a sample of the injection solution to calculate the percentage of injected dose per gram of tissue (% ID/g).

Stability experiments

The serum stability was determined by incubation of the ^{125}I-labeled GF-15 analogue in human serum at 37°C. Aliquots were taken at several points in time, and the degradation was stopped by precipitation of the serum proteins with acetonitrile. After incubation for 30 minutes at 0°C and a further centrifugation step the clear supernatant was analyzed by reverse-phase HPLC on a Chromolith Performance RP-18e 100 × 4.6 mm column using water and acetonitrile containing 0.1% trifluoroacetic acid as the eluent.

Isobologram analysis

For combination studies, data from MTT assays were converted into values representing the fraction of growth affected (FA) in drug-treated versus untreated cells and analyzed using CalcuSyn software program (Biosoft) based on the Chou-Talalay method. A combination index (CI) smaller than 0.9 indicates synergism, whereas 0.9 to 1.1 indicates additive and more than 1.1 antagonistic effects.

Statistical analysis

The statistical significance of differences observed in GF-15-treated versus control cell cultures and mice was determined using an unpaired Student *t* test or a 1-way ANOVA with Dunnett's Multiple Comparison Test for interkinetochore distances. Overall survival in animal studies was measured using the Kaplan–Meier method (*, $P > 0.01$; **, $P > 0.001$).

Results

GF-15 leads to multipolar mitosis induction in the upper nanomolar range

Recently, we have shown that 2′-modified derivatives of griseofulvin are more potent inducers of multipolar mitosis when compared with griseofulvin itself (21). Initial testing for the ability to inhibit centrosomal clustering was conducted in SCC114 cells, an oral squamous cell carcinoma line showing pronounced centrosome amplification (13, 18). GF-15 (2′-benzyloxy-2′-demethoxygriseofulvin) is significantly more potent with regard to the induction of spindle multipolarity than griseofulvin (Fig. 1A). The EC_{50} value of GF-15 for multipolar spindle induction was 900 nmol/L, corresponding to a 27-fold increase in activity compared with griseofulvin. Importantly, SCC114 cells that became resistant to GF-15 after long-term culture with increasing doses (0.2–1 μmol/L) of the compound over a period of 10 weeks, showed significantly less centrosome amplification and formed fewer multipolar spindles upon treatment with therapeutic doses (5 μmol/L) of the drug (Fig. 1B, Supplementary Fig. S1).

To test for the contribution of centrosome declustering to total multipolar mitosis induction after treatment with GF-

Figure 1. GF-15 is a potent and specific inducer of spindle multipolarity. A, chemical structures of griseofulvin and GF-15. SCC114 cells stably expressing α-tubulin were treated with increasing concentrations of griseofulvin or GF-15 for 24 hours. EC_{50} of spindle multipolarity was assessed by immunofluorescence microscopy. B, SCC114 cells resistant to GF-15 after long-term culture with increasing concentrations of GF-15 display significantly fewer cells with supernumerary centrosomes than wild-type SCC114. Centrosomes were counted in interphase cells by γ-tubulin/centrin coimmunostaining. **, $P < 0.001$. C, in PC-3 prostate cancer cells, GF-15 induces centrosomal declustering (Declustered) in cells with amplified centrosomes and spindle multipolarity by other means (aberrant) in cells with regular centrosome content in a concentration-dependent manner. The dashed line depicts the overall percentage of PC-3 cells with centrosome amplification. D, spindle phenotypes of PC-3 cells upon treatment with vehicle only (D′, D′′) or GF-15 (D′′′, D′′′′) according to their regular versus amplified centriole content. Cells were treated with GF-15 or vehicle only for 24 hours, spindle poles were counted by γ-tubulin staining, centrioles by centrin staining. Insets show enlargements of centrin signals at each spindle pole. All scale bars represent 5 μm. E, GF-15 reduces spindle tension in PC-3 cells exposed to GF-15 (1 μmol/L; 24 hours). Interkinetochore distances from multipolar and bipolar spindles (table) are given as mean and SD. Cells were stained for CREST (green), HEC1 (red), γ-tubulin (purple), and DNA (4′, 6-diamidino-2-phenylindole, DAPI; blue; right). Sister kinetochores were identified by spatial correlation of HEC1 and CREST as a marker of the interkinetochore space. Distances between corresponding HEC1 signals were measured. F, GF-15 triggers the spindle assembly checkpoint. PC-3 cells were exposed to DMSO control, taxol (10 nmol/L) as a positive control, and GF-15 (0.75 μmol/L and 1.5 μmol/L, respectively) for 24 hours and stained for α-tubulin, BubR1, and DAPI. BubR1 staining of kinetochores indicates an active spindle assembly checkpoint. G, the effects of increasing concentrations of griseofulvin (GF, left) or GF-15 (right), respectively, on tubulin polymerization were measured by relative fluorescence intensity. All quantitative data shown are the mean ± SD of 3 independent experiments.

Published OnlineFirst August 31, 2012; DOI: 10.1158/0008-5472.CAN-12-2026

15, the PC-3 prostate carcinoma cell line, which harbors supernumerary centrosomes in 28 ± 4% of the cells, was treated with increasing concentrations of the drug for 24 hours (Fig. 1C). Intriguingly, at the highest analyzable concentration (1.5 μmol/L), GF-15 induced centrosome declustering—as defined by the detection of 2 centrioles at each spindle pole of multipolar mitoses (Fig. 1D)—in 27 ± 4% of the cells, thereby closely matching the total percentage of cells with supernumerary centrosomes. At the lowest concentration tested (0.375 μM), multipolarity induction was mostly due to inhibition of centrosomal clustering. With increasing doses of GF-15, the contribution of multipolarity induction by other means gradually increased. This phenomenon was arbitrarily termed "aberrant," defined by the presence of centrioles at only 2 spindle poles despite cells were undergoing multipolar mitoses. From these results, it may be concluded that the mechanisms responsible for holding supernumerary centrosomes together might be similar to the forces that bundle microtubules into a bipolar spindle array in cells with a regular centrosome content. However, differential sensitivities of both mechanisms may provide a therapeutic window to preferentially target centrosome clustering at lower dose levels.

Recently, we and others have shown that spindle tension is required for centrosomal clustering (19, 20). To directly measure spindle tension, we determined interkinetochore distances in mitotic PC-3 cells with either bipolar or multipolar spindles after treatment with 1 μmol/L GF-15 for 24 hours (Fig. 1E). Tension across sister kinetochores was substantially reduced by GF-15, as indicated by shorter interkinetochore distances in multipolar metaphase cells. To a lesser but still significant extent, interkinetochore distances were also reduced in metaphase cells that remained bipolar despite treatment with GF-15. If spindle tension is disturbed, the spindle assembly checkpoint cannot get sufficiently satisfied during metaphase and BubR1 should remain at affected kinetochores. As shown in Fig. 1F, kinetochores of multipolar metaphases in GF-15-treated cells stained positive for BubR1 similarly to cells exposed to low-dose taxol, used as a positive control. In contrast, BubR1 was absent from bipolar metaphases in vehicle-treated control cells. Moreover, no MAD2 signal as a marker for disturbed spindle attachment could be detected at kinetochores of GF-15 induced multipolar metaphases, in contrast to kinetochores of cells treated with nocodazole as a positive control (data not shown). These findings show that GF-15 reduces spindle tension and thereby activates the spindle assembly checkpoint, but does not disturb microtubule attachment to kinetochores. This corroborates earlier findings showing that reduced spindle tension after siRNA-mediated depletion of kinetochore and spindle components leads to the formation of multipolar spindles (19, 20).

Effects of griseofulvin and GF-15 on tubulin polymerization *in vitro*

To exclude the hypothesis that loss of spindle tension upon GF-15 exposure is merely a consequence of tubulin depolymerization, the effects of griseofulvin and GF-15 on the polymerization of purified porcine brain tubulin into microtubules *in vitro* were analyzed using a fluorescence assay (26). Corroborating earlier data, inhibition of brain tubulin polymerization required very high concentrations of griseofulvin (27, 28). Similarly, the GF-15 concentrations needed for inhibition of tubulin polymerization (25 μmol/L) were about 25-fold above those required for induction of spindle multipolarity (Fig. 1G).

GF-15 causes multipolar anaphases and cell death in cells with supernumerary centrosomes

Cells with supernumerary centrosomes only rarely undergo multipolar divisions. Instead they pass through a transient multipolar intermediate state followed by centrosome clustering and bipolar anaphase (14, 15). To ascertain that GF-15 indeed induces multipolar cell divisions and subsequent cell death in cells with supernumerary centrosomes, HeLa cells were induced to contain extra centrioles by conditional overexpression of PLK4 (28; Supplementary Fig. S2). In these cells, in the second cell cycle after centriole overduplication, supernumerary centrioles disengage before duplication and multipolar intermediates are common in the following mitosis (14, 29). Treatment of HeLa–PLK4 cells with increasing concentrations of GF-15 for 24 hours, starting 48 hours after induction of PLK4 expression by addition of doxycycline, led to a dose-dependent, marked increase in the frequency of multipolar anaphases with declustered centrosomes (Fig. 2A and B; Supplementary Fig. S3). In addition, compared with uninduced cells, GF-15 preferentially decreased the viability of HeLa cells after PLK4-induced centriole overduplication (Fig. 2C).

GF-15 is active against a broad spectrum of cancer cell lines *in vitro*

Next, we examined the effect of GF-15 on the growth of several different cancer cell lines. GF-15 exhibits potent cytotoxicity in a concentration-dependent manner against a broad spectrum of tumor cell types including colon, cervix, glioblastoma, pancreas, leukemia, and myeloma-derived cell lines (Fig. 3A). As compared with solid tumor cell lines, MM and leukemia cell lines were particularly susceptible to the cytotoxic and antiproliferative effect of GF-15 with IC_{50} values ranging from 1 to 2.5 μmol/L. In contrast, GF-15 did not induce significant cytotoxicity in nonmalignant control cell lines (Fig. 3A) or PBMCs from healthy volunteers even after stimulation with phytohemagglutinin (PHA), providing an overall selectivity index of 10- to 30-fold when compared with IC_{50} values of cancer cell lines (Fig. 3B). These data suggest that GF-15 exhibits both potent and selective cytotoxicity against malignant cells.

GF-15 is rapidly eliminated *in vivo*

Derived from its parental molecule griseofulvin, GF-15 has been modified at the 2′-position (Fig. 1A). We therefore sought to analyze the *in vivo* stability and pharmacokinetics of this new compound. By introducing a *p*-iodobenzyl group in the 2′-position of the griseofulvin molecule, we generated a ^{125}I-labeled GF-15-analogue. HPLC analysis showed only slow degradation of this molecule in human serum with a half-life

Published OnlineFirst August 31, 2012; DOI: 10.1158/0008-5472.CAN-12-2026

of 48 hours at 37°C. The cleavage products resulting from degradation are presumably 4-iodobenzyl alcohol and griseofulvic acid, consistent with the analogue undergoing hydrolysis (data not shown). After i.v. application of trace amounts of this analogue, rapid renal clearance was observed within the first 6 hours after injection (Fig. 3C and D). In light of the clearance data and the poor solubility of GF-15 at higher concentrations, we went on to investigate its *in vivo* efficacy after intraperitoneal application.

GF-15 exhibits *in vivo* antitumor activity in xenograft mouse models

In view of the potent and selective *in vitro* activity of GF-15 against different cancer cell lines, we next examined the *in vivo* effect of GF-15 on human tumor growth in immunodeficient mice. Two cohorts, each consisting of 30 immunodeficient beige-nude-Xid mice were inoculated with either 3×10^6 OPM2 myeloma or HT29 colon cancer cells s.c. in the right flank. Treatment with a daily dose of 20 mg/kg (10 mice per cell line) or 100 mg/kg (10 mice per cell line) intraperitoneally 5 days per week for 2 weeks was started when tumors became palpable. Ten mice per cell line served as a control cohort and received intraperitoneal injections of the vehicle alone. GF-15 treatment decreased tumor growth in all cohorts of treated mice with a greater effect in the group that received 100 mg/kg intraperitoneally (Figs. 4A, Supplementary Fig. S4). Kaplan–Meier and log-rank analysis revealed a significant prolongation of survival for the GF-15-treated mice inoculated with OPM2 myeloma cells compared with the vehicle-treated controls (log-rank $P < 0.001$; Fig. 4B). For mice inoculated with HT29 colon cancer cells survival analysis was not feasible because tumors in the control group rapidly became exulcerated and therefore had to be sacrificed according to institutional regulations. The toxicity profile of GF-15 seems to be quite favorable as body weight was not affected by treatment with GF-15 compared with untreated controls (Fig. 4C). Importantly, examination of histologic tumor sections revealed a dose-dependent, significant increase of aberrant and multipolar mitoses in the GF-15-treated mice compared with controls ($P < 0.01$ for 20 mg/kg, $P < 0.001$ for 100 mg/kg; Fig. 4D and E). In addition, GF-15 significantly increased the mitotic index in treated tumors versus controls (Supplementary Fig. S5).

Induction of spindle multipolarity, mitotic arrest and apoptosis by GF-15

As already depicted in Fig. 3A, myeloma cell lines are among those tumor types with particular susceptibility to GF-15. Because myeloma cells are known to harbor supernumerary centrosomes (3–5), we used MM cells as a model system for further in-depth analyses. Similar to OPM2, RPMI-8226, NCI-

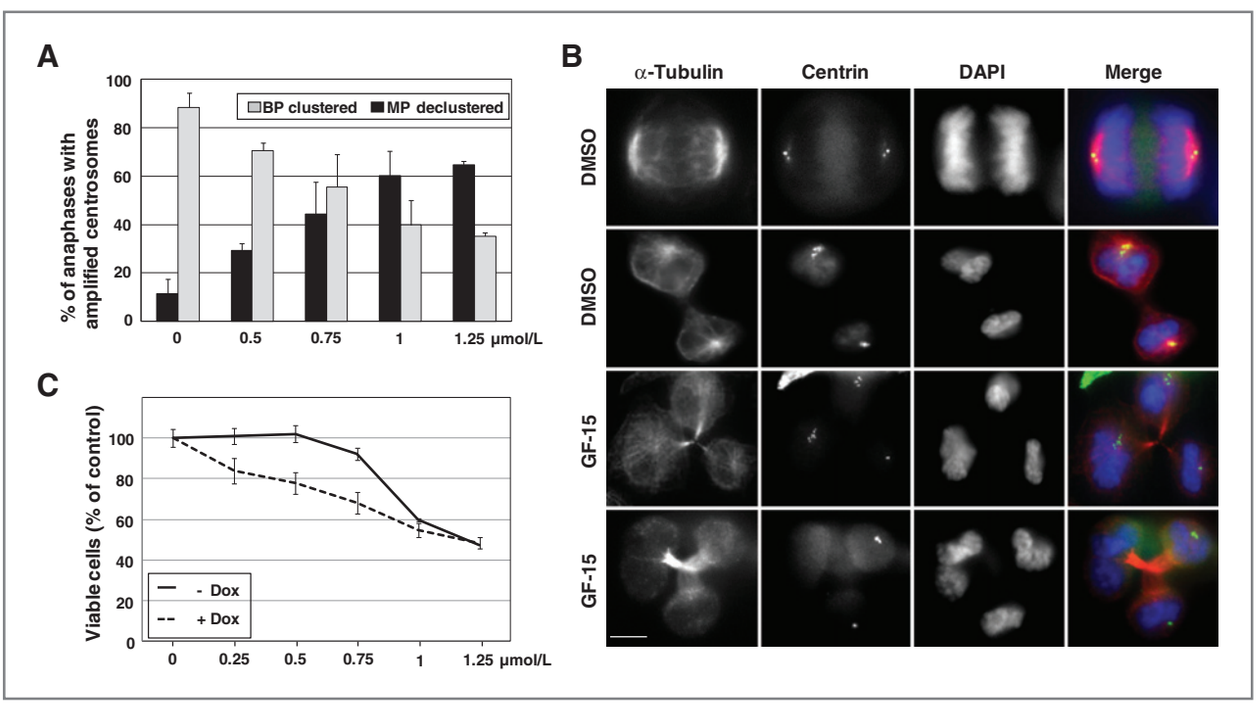

Figure 2. Centriole amplification sensitizes cells to treatment with GF-15. A, dose-dependent declustering of amplified centrosomes and induction of multipolar (MP) versus clustered bipolar (BP) cell divisions by GF-15 in HeLa cells conditionally expressing PLK4, stained for α-tubulin (red), centrin (green), and DNA (blue; B). At least 100 anaphases of cells with amplified centrioles were counted for each concentration. The first panel from the top shows a regular bipolar cell division without centriole amplification compared with the second panel with amplified centrioles clustered into bipolar spindle poles. The third panel displays partial declustering of amplified centrioles resulting in tripolar cell division, whereas the fourth panel represents aberrant multipolarity in a cell without amplified centrioles (second centriole at lower pole out of focus). See also Supplementary Fig. S3. Scale bar, 5 μm. C, viable cells were assessed by MTT cleavage during the last 4 hours of 48-hour cultures of HeLa–PLK4 cells with and without doxycycline (±Dox, 48 hours) with increasing concentrations of GF-15. All quantitative data shown are the mean ± SD of 3 independent experiments conducted in triplicate.

Published OnlineFirst August 31, 2012; DOI: 10.1158/0008-5472.CAN-12-2026

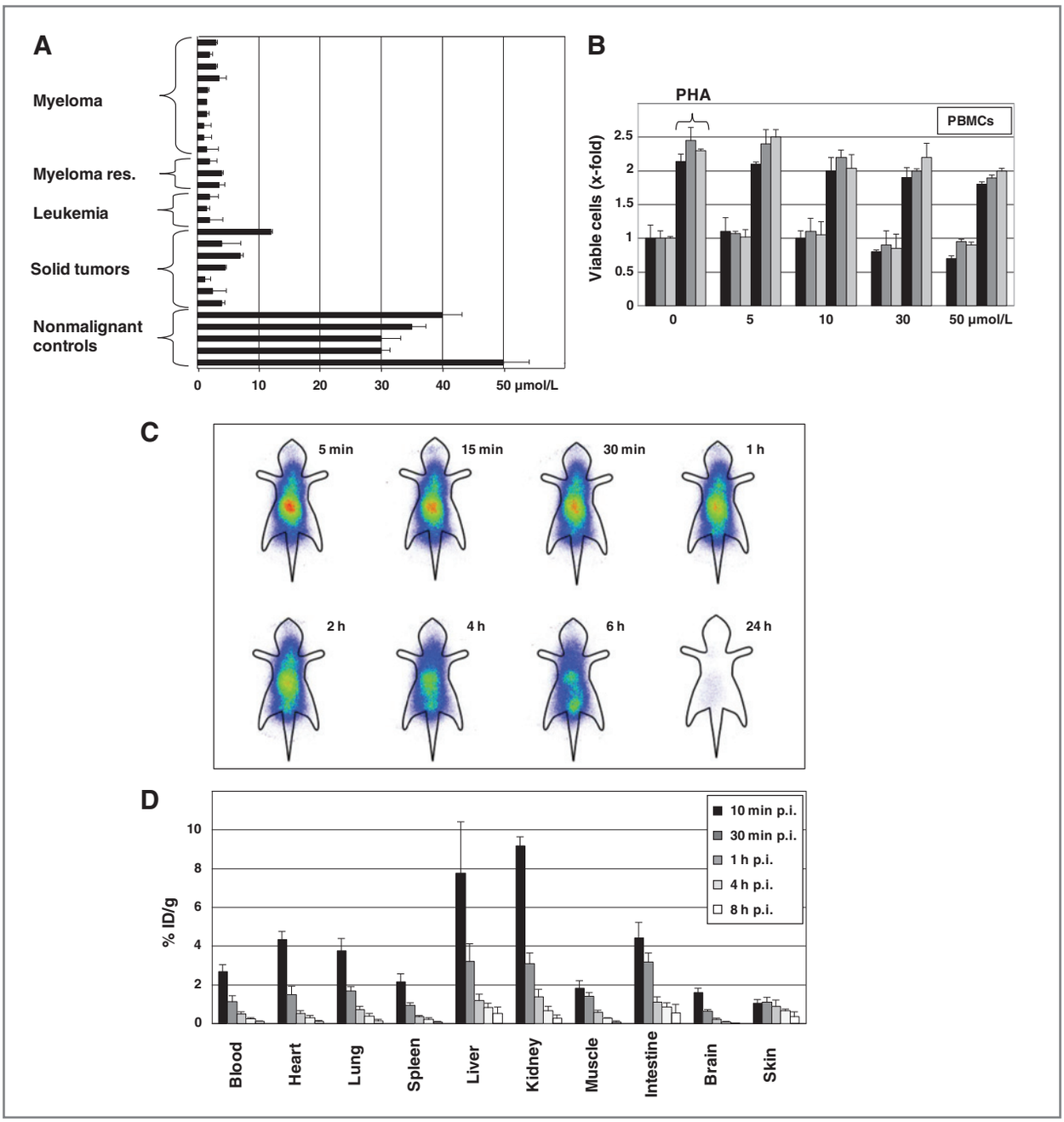

Figure 3. GF-15 selectively inhibits growth of tumor cells *in vitro* and *in vivo*. A, IC_{50} values of cell lines of indicated origins. Unless otherwise indicated, viable cells were measured by MTT cleavage during the last 4 hours of 48-hour cultures. Data shown are the mean ± SD of experiments conducted in triplicate. B, PBMCs of 3 healthy donors stimulated with PHA do not show significant toxicity upon treatment with indicated concentrations of GF-15. PBMCs were incubated with PHA 24 hours before exposure to GF-15 for 48 hours. Column colors represent corresponding PBMC samples with or without PHA, respectively. Viable cells are expressed as x-fold of respective control. C, whole-body scintigraphic images of NMRI mice at indicated times after intravenous injection of a ^{125}I-labeled GF-15 analogue. D, biodistribution of a ^{131}I-labeled GF-15 analogue at different times after intravenous administration to NMRI mice ($n = 12$). Data are expressed as mean %ID/g ± SD of each time point. ID, injected dose; p.i., postinjection. All quantitative data shown are the mean ± SD of 3 independent experiments.

H929, OPM1, and KMS12BM myeloma cells, myeloma cell lines resistant to doxorubicin (Dox40), melphalan (LR5), and dexamethasone (MM1.R) are susceptible to GF-15 as well (Fig. 5A and B). Moreover, primary myeloma cells freshly isolated from the bone marrow of 3 (out of 10) heavily pretreated patients with relapsed myeloma showed marked cytotoxic effects upon treatment with GF-15. Lack of efficacy in the remaining 7 myeloma samples was most likely due to lack of proliferation, a

Published OnlineFirst August 31, 2012; DOI: 10.1158/0008-5472.CAN-12-2026

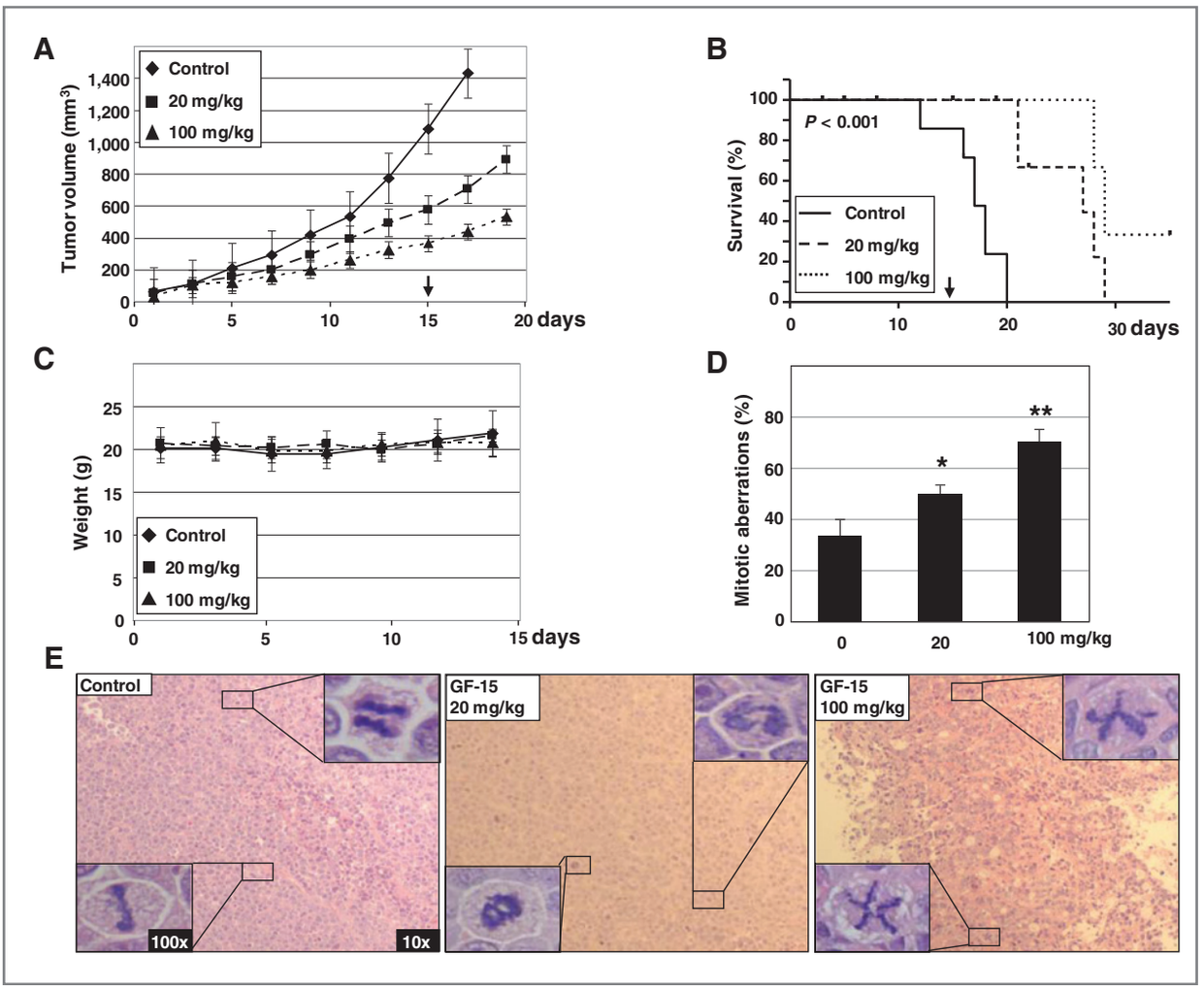

Figure 4. GF-15 decreases tumor growth, prolongs survival, and induces mitotic aberrations in a MM xenograft mouse model. A, beige-nude Xid mice were subcutaneously inoculated in the right flank with 3×10^6 OPM2 cells. Treatment by intraperitoneal injection (vehicle alone or indicated concentrations of GF-15) was started when tumors were measurable. Arrows indicate treatment stop. Tumor burden was measured every alternating day using an electronic caliper. Tumor volume is presented as means ± SE. B, survival was evaluated using Kaplan–Meier curves and log-rank analysis. C, body weight was evaluated 3 times per week. Data shown are the mean ± SD. *, $P < 0.01$; **, $P < 0.001$. D, in hematoxylin and eosin-stained tumor sections ($n = 3$ per cohort), at least 200 mitotic cells were analyzed for mitotic aberrations. E, dose-dependent effects of GF-15 on mitotic figures. Paraffin-embedded sections of tumor tissue, explanted 24 hours after last treatment, were hematoxylin and eosin-stained and analyzed by light microscopy. Representative microscopic images are shown.

common phenomenon of primary myeloma cells in tissue culture. This was in stark contrast to their corresponding proliferating BMSCs, which displayed virtually no cytotoxicity when exposed to GF-15 (Fig. 5C). Likewise, after 24 hours of treatment with 3 μmol/L GF-15, no significant induction of spindle multipolarity could be detected in mitotic primary BMSCs, whereas more than 80% of mitoses were multipolar in NCI H929, OPM2, and RPMI 8226 cells (Fig. 5D). To examine the effect of multipolar mitosis induction on cell-cycle progression, starvation-synchronized OPM2 cells were exposed to GF-15, stained with propidium iodide, and subsequently analyzed by flow cytometry. GF-15 induced a pronounced G_2–M cell-cycle arrest within 12 hours of treatment followed by an increase of the sub-G_1 population compared with mock-treated cells (Fig. 5E, top panel). Indicating the induction of apoptosis, the increase of the sub-G_1 population was concentration-dependent (Fig. 5E, bottom panel), analogous to the effect of griseofulvin in SCC114 cells (13). To further verify apoptotic cell death triggered by GF-15, protein profiling in GF-15-treated MM cells showed dose-dependent cleavage of caspase-8, caspase-9, caspase-3, and PARP (Fig. 5F). Cleavage fragments of these proteins became detectable at 0.5 μmol/L and strongly increased at 3 μmol/L of GF-15. Importantly, exposure of primary BMSCs to 3 μmol/L of GF-15 for 24 hours did not induce activation of effector caspases-3 and -7 compared with OPM2 cells (Fig. 5G).

GF-15 inhibits myeloma cell growth triggered by BMSCs

In addition to the effects mediated by growth factors and cytokines within the myeloma bone marrow

Published OnlineFirst August 31, 2012; DOI: 10.1158/0008-5472.CAN-12-2026

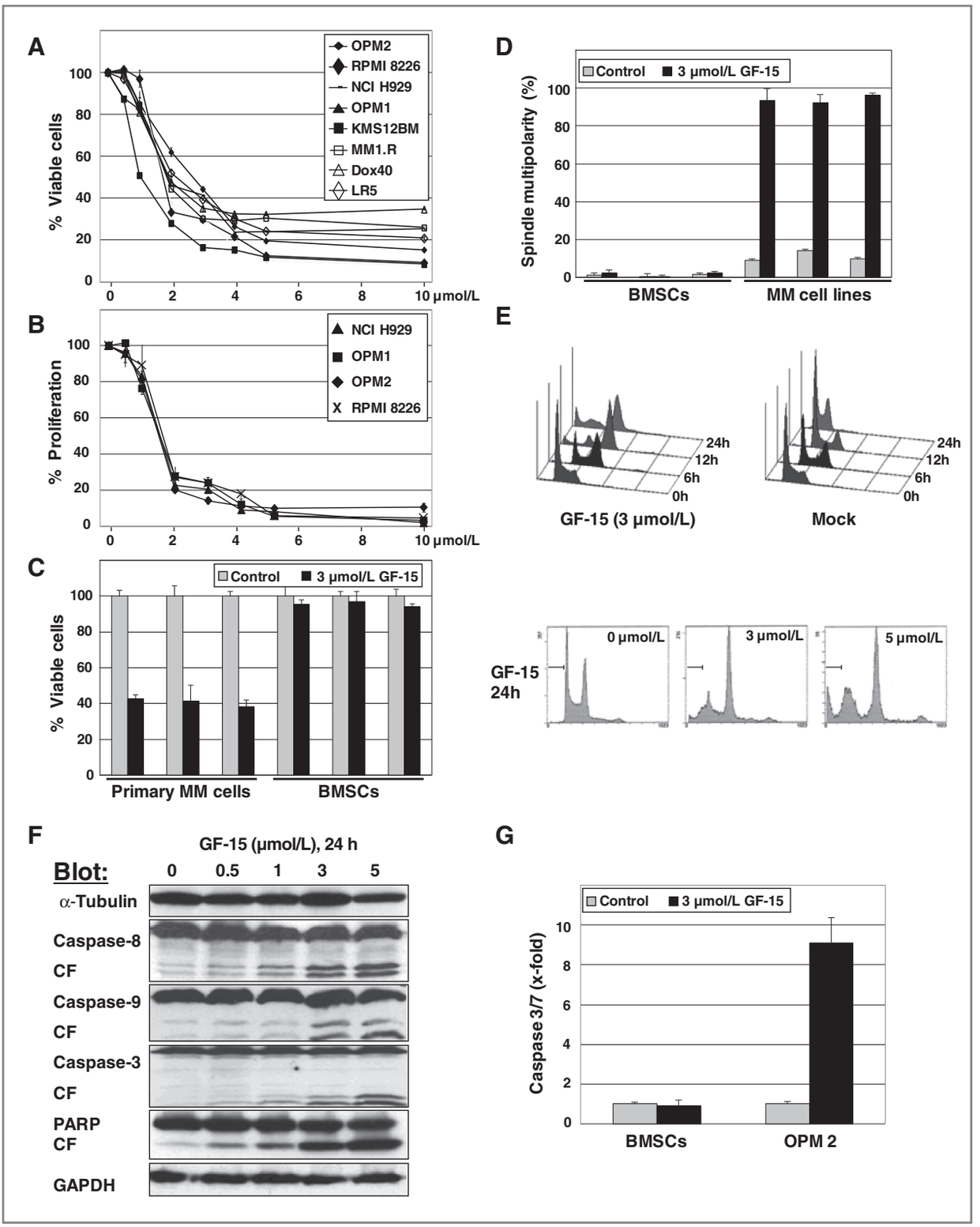

Figure 5. GF-15 specifically induces growth inhibition, spindle multipolarity, cell-cycle arrest, and apoptosis in MM cells. A and B, dose-related effects of GF-15 on cell survival (48 hours; A) and proliferation (24 hours; B) on indicated MM cell lines. Cell proliferation was assessed by uptake of [^{3}H]-thymidine during the last 8 hours of 24-hour cultures. C, GF-15 differentially inhibits cell survival of primary cells from MM patients compared with patient BMSCs. D, GF-15 selectively induces multipolar mitotic spindles in MM cells (NCI H929, OPM2, RPMI 8226; left to right) compared with primary BMSCs from 3 MM patients. At least

Published OnlineFirst August 31, 2012; DOI: 10.1158/0008-5472.CAN-12-2026

microenvironment, direct myeloma–stroma contact also triggers tumor cell growth and mediates drug resistance. We therefore evaluated the effect of GF-15 on myeloma cell proliferation induced by the stimulatory effect of BMSCs (Fig. 6A and B). Binding of OPM2 or RPMI-8226 cells to primary BMSCs triggered increased myeloma cell proliferation, which was completely abrogated by GF-15. Importantly, as also shown in Figs. 5C and D, GF-15 did not impact on BMSCs, as determined by MTT assays and spindle polarity analysis.

Evaluation of combinations of GF-15 with other antimyeloma agents

Clinical experience in the therapeutic management of MM supports the notion that drug combinations can induce higher response rates when compared with single-agent treatment (23, 30). We therefore evaluated the effects of combinations of GF-15 with other established anti-MM drugs on the viability of MM cells. Specifically, GF-15 was combined with conventional agents (melphalan) as well as with more recently developed compounds (bortezomib). Although GF-15 together with bortezomib resulted in additive effects according to isobologram analysis (e.g., CI = 0.98 for 1.5 μmol/L GF-15 with 1.5 nmol/L bortezomib), the combination with melphalan led to a marked abrogation of GF-15 induced cytotoxicity (CI = 1.4 for 3 μmol/L GF-15 with 5 μmol/L melphalan, Fig. 6C). This is consistent with an S-phase arrest induced by the DNA-damaging drug melphalan, thereby preventing entry into mitosis of melphalan-exposed cells and underlines the specificity of GF-15 for cells in G_2–M phase of the cell cycle.

Discussion

We show here that GF-15, a derivative of griseofulvin, leads to multipolar cell division, loss of spindle tension, centrosomal declustering, and subsequent tumor-specific cell death both in tissue culture and in xenograft mouse models.

Griseofulvin has been used for many years for the treatment of dermatophyte infections (31). Mechanistically, it inhibits mitosis in sensitive fungi (32) and mammalian cells (33, 34) but whether mitotic arrest is a consequence of microtubule depolymerization or some other action on microtubules in both fungi and human cells is still unclear (27, 28, 33, 35). Interestingly, in a recent comparison of analogues in fungal and mammalian cells we found that GF-15 was less active against dermatophytes than griseofulvin (36). Although griseofulvin has been reported to bind to mammalian brain tubulin and to inhibit microtubule polymerization *in vitro*, it does so only at concentrations significantly higher than those needed for spindle multipolarity induction in cancer cells (13, 35). Also, whether griseofulvin binds to tubulin directly or to microtubule-associated proteins remains unclear (27, 35, 37, 38). It was reported more than 30 years ago that griseofulvin treatment induces spindle multipolarity with each mitotic center containing 2 centrioles in HeLa cells in the absence of significant spindle microtubule depolymerization (33). In accordance with these findings, our data show that griseofulvin significantly inhibits polymerization of purified tubulin only at the highest concentration tested (100 μmol/L), although induction

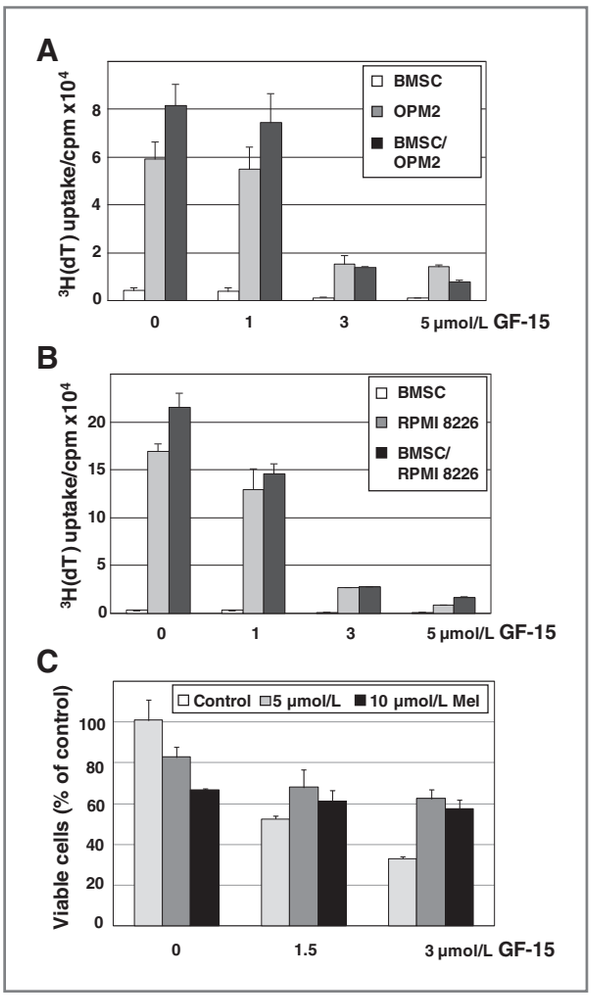

Figure 6. GF-15 abrogates the growth advantage of tumor cells conferred by adhesion to primary BMSCs. A and B, indicated MM cell lines were cultured with or without primary BMSCs. GF-15 was added at indicated concentrations and proliferation was measured by [^{3}H]-thymidine uptake during the last 8 hours of 24-hour cultures. C, cotreatment of MM cells with melphalan partially abrogates the growth inhibitory effects of GF-15. OPM2 cells were treated with indicated concentrations of GF-15 with or without 5 or 10 μmol/L of melphalan. All quantitative data shown are the mean ± SD of 3 independent experiments conducted in triplicate.

200 mitotic cells were counted for spindle polarity after staining for γ-tubulin, Eg5, and 4′, 6-diamidino-2-phenylindole. E, synchronized OPM2 cells arrest in G_2–M phase upon treatment with GF-15 followed by an increase of the sub-G_1 population (top). The increase of the sub-G_1 population is dose-dependent (bottom). OPM2 cells were exposed for indicated times to indicated concentrations of GF-15 and subsequently stained with propidium iodide after ethanol fixation. F, GF-15 triggers apoptotic cell death in MM cells. OPM2 cells were exposed to indicated concentrations of GF-15 for 24 hours, followed either by immunoblot analysis of lysates with indicated antibodies or ELISA-based assessment of activation of effector caspases-3 and -7 (G). Identical treatment of BMSCs showed no significant induction of caspase 3/7 activation compared with OPM2 cells. Results are expressed as x-fold of control. CF, cleaved form of respective protein. All quantitative data shown are the mean ± SD of 3 independent experiments conducted in triplicate.

Published OnlineFirst August 31, 2012; DOI: 10.1158/0008-5472.CAN-12-2026

of spindle multipolarity by griseofulvin occurred at an EC_{50} of 25 μmol/L in SCC114 cells. Similarly, GF-15 inhibits tubulin polymerization only at concentrations of or above 25 μmol/L, whereas the EC_{50} value for multipolar spindle induction was 900 nmol/L in SCC114 cells for this compound. These findings suggest that induction of spindle multipolarity by griseofulvin and its analog GF-15 is not sufficiently explained by their inhibitory action on tubulin polymerization.

It has recently been shown that cells with supernumerary centrosomes pass through a transient multipolar spindle intermediate state before centrosome clustering and subsequent bipolar anaphase occur (14, 15). At low concentrations GF-15 leads to multipolar metaphases with centrioles at each pole in cells with extra centrioles. At higher concentrations spindle multipolarity with acentrosomal spindle pole formation is induced. This is consistent with the concept that clustering extra centrosomes in cancer cells might be mechanistically related to focusing microtubules into a bipolar spindle array in normal cells. Analysis of GF-15-treated HeLa cells conditionally overexpressing PLK4 revealed that spindle multipolarity is carried on into anaphase/telophase with centrioles at each pole in a substantial proportion of cells with PLK4-induced centriole amplification. Moreover, treatment with GF-15 increased the death rates of HeLa cells after induction of PLK4 expression, suggesting that GF-15 preferentially kills cells with amplified centrioles.

Recent genome-wide RNAi screens in cells containing supernumerary centrosomes suggest that only an intact spindle assembly checkpoint allows for sufficient time for centrosomal clustering to occur and that spindle tension is necessary for clustering of supernumerary centrosomes into a bipolar mitotic spindle array (19, 20). Determination of spindle tension in mitotic cells revealed that tension across sister kinetochores was substantially reduced by GF-15 in both multipolar metaphase cells and metaphase cells that remained bipolar despite treatment with GF-15. In addition to microtubule depolymerization or stabilization at higher concentrations, most microtubule-interacting drugs, including griseofulvin, have been proposed to exert their effects by suppressing microtubule dynamics (35, 38). Interestingly, interference with microtubule dynamics has been described to cause loss of spindle tension across kinetochores (39, 40). Therefore, it is conceivable that GF-15 inhibits microtubule dynamic instability with subsequent loss of spindle tension, centrosome declustering in cells with supernumerary centrosomes, multipolar cell division, and ultimately cell death.

For GF-15, the EC_{50} value for multipolar spindle induction *in vitro* was 900 nmol/L in SCC114 cells, corresponding to a 27-fold increased activity compared with griseofulvin itself. Also, whereas griseofulvin inhibits cell proliferation only weakly with half-maximal inhibition occurring at 25 μmol/L (13), GF-15 led to inhibition of tumor cell growth *in vitro* at IC_{50} values of 1 to 3 μmol/L, with almost no impact on the viability of nonmalignant control cell lines. Similarly, although 3 μmol/L GF-15 effectively decreased the viability of primary patient myeloma cells, the drug induced neither spindle multipolarity nor cell death in primary BMSCs or primary PBMCs even after mitogenic stimulation. *In vivo*, GF-15 was well tolerated and effective in mouse myeloma and colon cancer xenograft models, as evidenced by significant inhibition of tumor growth, the induction of spindle multipolarity in tumor xenograft cells and prolonged survival in mice treated with either 20 or 100 mg/kg GF-15 intraperitoneally daily for 5 days a week. Because GF-15 is only poorly soluble in water and its biologic half-life is short with little drug left 1 hour after administration, it is expected that optimization of medicinal chemistry and application schedules will lead to a further improvement of the drugs potency and of this novel therapeutic strategy in general.

In summary, we have shown that GF-15 potently inhibits tumor cell growth *in vitro* and *in vivo*. From a mechanistic point of view our data reveal that GF-15 reduces spindle tension, possibly via inhibition of microtubule dynamic instability, leading to spindle multipolarity in cells with supernumerary centrosomes, similar to what has been described for the siRNA-mediated depletion of several spindle and kinetochore components (19, 20). These observations, coupled with GF-15's lack of major toxicity in a preclinical mouse model and the lack of significant toxicity of griseofulvin in humans, provide the framework for further clinical development of GF-15 in particular and centrosomal cluster inhibitors in general, directed at improving patient outcome.

Disclosure of Potential Conflicts of Interest

K.C. Anderson is an ACS Clinical Research Professor. No potential conflicts of interest were disclosed by the other authors.

Authors' Contributions

Conception and design: M.S. Raab, I. Breitkreutz, W. Mier, M.H. Clausen, A. Krämer
Development of methodology: I. Breitkreutz, M.H. Ronnest, W. Mier, A. Krämer
Acquisition of data (provided animals, acquired and managed patients, provided facilities, etc.): M.S. Raab, I. Breitkreutz, M.H. Ronnest, B. Leber, L. Weiz, G. Konotop, K. Podar, J. Fruehauf, F. Nissen, W. Mier, U. Haberkorn
Analysis and interpretation of data (e.g., statistical analysis, biostatistics, computational analysis): M.S. Raab, I. Breitkreutz, M.H. Ronnest, B. Leber, F. Nissen, M.H. Clausen, A. Krämer
Writing, review, and/or revision of the manuscript: M.S. Raab, I. Breitkreutz, M.H. Ronnest, T.O. Larsen, P.J. Hayden, K. Podar, J. Fruehauf, W. Mier, H. Goldschmidt, K.C. Anderson, M.H. Clausen, A. Krämer
Administrative, technical, or material support (i.e., reporting or organizing data, constructing databases): I. Breitkreutz, A.D. Ho
Study supervision: A. Krämer
Performing experiments: S. Anderhub

Acknowledgments

The authors thank Ingrid Hoffmann, PhD, German Cancer Research Center, for providing the conditional HeLa-PLK4 cell line and J. Salisbury (Rochester) for the centrin antibody. The authors also thank Anja Baumann for excellent technical assistance.

Grant Support

This work was supported by a grant of the Max-Eder-Program, Deutsche Krebshilfe (M.S. Raab); the Hopp-Foundation (H. Goldschmidt); the DFG (A. Krämer); a Deutsche Krebshilfe grant (M.S. Raab and A. Krämer); the Tumorzentrum Heidelberg/Mannheim (A. Krämer); the Danish Research Council (ref. 274-07-0561; M.H. Ronnest, T.O. Larsen, and M.H. Clausen); the Danish Cancer Society and Karen Krieger Fonden (M.H. Clausen); the NIH grants RO CA50947, PO-1 CA78378, and P50 CA100707 (K.C. Anderson).

The costs of publication of this article were defrayed in part by the payment of page charges. This article must therefore be hereby marked *advertisement* in accordance with 18 U.S.C. Section 1734 solely to indicate this fact.

Received May 29, 2012; revised August 6, 2012; accepted August 21, 2012; published OnlineFirst August 31, 2012.

Published OnlineFirst August 31, 2012; DOI: 10.1158/0008-5472.CAN-12-2026

References

1. Doxsey S. Re-evaluating centrosome function. Nat Rev Mol Cell Biol 2001;2:688–98.
2. Krämer A, Neben K, Ho AD. Centrosome replication, genomic instability and cancer. Leukemia 2002;16:767–75.
3. Chng WJ, Ahmann GJ, Henderson K, Santana-Davila R, Greipp PR, Gertz MA, et al. Clinical implication of centrosome amplification in plasma cell neoplasm. Blood 2006;107:3669–75.
4. Chng WJ, Braggio E, Mulligan G, Bryant B, Remstein E, Valdez R, et al. The centrosome index is a powerful prognostic marker in myeloma and identifies a cohort of patients that might benefit from aurora kinase inhibition. Blood 2008;111:1603–9.
5. Maxwell CA, Keats JJ, Belch AR, Pilarski LM, Reiman T. Receptor for hyaluronan-mediated motility correlates with centrosome abnormalities in multiple myeloma and maintains mitotic integrity. Cancer Res 2005;65:850–60.
6. Lingle WL, Lutz WH, Ingle JN, Maihle NJ, Salisbury JL. Centrosome hypertrophy in human breast tumors: implications for genomic stability and cell polarity. Proc Natl Acad Sci U S A 1998;95:2950–5.
7. Pihan GA, Purohit A, Wallace J, Knecht H, Woda B, Quesenberry P, et al. Centrosome defects and genetic instability in malignant tumors. Cancer Res 1998;58:3974–85.
8. Nigg EA. Centrosome aberrations: cause or consequence of cancer progression? Nat Rev Cancer 2002;2:815–25.
9. Neben K, Giesecke C, Schweizer S, Ho AD, Krämer A. Centrosome aberrations in acute myeloid leukemia are correlated with cytogenetic risk profile. Blood 2003;101:289–91.
10. Krämer A, Schweizer S, Neben K, Giesecke C, Kalla J, Katzenberger T, et al. Centrosome aberrations as a possible mechanism for chromosomal instability in non-Hodgkin's lymphoma. Leukemia 2003;17:2207–13.
11. Levine DS, Sanchez CA, Rabinovitch PS, Reid BJ. Formation of the tetraploid intermediate is associated with the development of cells with more than four centrioles in the elastase-simian virus 40 tumor antigen transgenic mouse model of pancreatic cancer. Proc Natl Acad Sci U S A 1991;88:6427–31.
12. Pihan GA, Purohit A, Wallace J, Malhotra R, Liotta L, Doxsey SJ. Centrosome defects can account for cellular and genetic changes that characterize prostate cancer progression. Cancer Res 2001;61:2212–9.
13. Rebacz B, Larsen TO, Clausen MH, Rønnest MH, Löffler H, Ho AD, et al. Identification of griseofulvin as an inhibitor of centrosomal clustering in a phenotype-based screen. Cancer Res 2007;67:6342–50.
14. Ganem NJ, Godinho SA, Pellman D. A mechanism linking extra centrosomes to chromosomal instability. Nature 2009;460:278–82.
15. Silkworth WT, Nardi IK, Scholl LM, Cimini D. Multipolar spindle pole coalescence is a major source of kinetochore mis-attachment and chromosome mis-segregation in cancer cells. PLoS One 2009;4:e6564.
16. Ring D, Hubble R, Kirschner M. Mitosis in a cell with multiple centrioles. J Cell Biol 1982;94:549–56.
17. Brinkley BR. Managing the centrosome numbers game: from chaos to stability in cancer cell division. Trends Cell Biol 2001;11:18–21.
18. Quintyne NJ, Reing JE, Hoffelder DR, Gollin SM, Saunders WS. Spindle multipolarity is prevented by centrosomal clustering. Science 2005;307:127–9.
19. Kwon M, Godinho SA, Chandhok NS, Ganem NJ, Azioune A, Thery M, et al. Mechanisms to suppress multipolar divisions in cancer cells with extra centrosomes. Genes Dev 2008;22:2189–203.
20. Leber B, Maier B, Fuchs F, Chi J, Riffel P, Anderhub S, et al. Proteins required for centrosome clustering in cancer cells. Sci Transl Med 2010;2:33ra38.
21. Rønnest MH, Rebacz B, Markworth L, Terp AH, Larsen TO, Krämer A, et al. Synthesis and structure-activity relationship of griseofulvin analogues as inhibitors of centrosomal clustering in cancer cells. J Med Chem 2009;52:3342–7.
22. Podar K, Tai YT, Davies FE, Lentzsch S, Sattler M, Hideshima T, et al. Vascular endothelial growth factor triggers signaling cascades mediating multiple myeloma cell growth and migration. Blood 2001;98:428–35.
23. Hideshima T, Chauhan D, Hayashi T, Podar K, Akiyama M, Mitsiades C, et al. Antitumor activity of lysophosphatidic acid acyltransferase-beta inhibitors, a novel class of agents, in multiple myeloma. Cancer Res 2003;63:8428–36.
24. Krämer A, Mailand N, Lukas C, Syljuåsen RG, Wilkinson CJ, Nigg EA, et al. Centrosome-associated Chk1 prevents premature activation of cyclin-B-Cdk1 kinase. Nat Cell Biol 2004;6:884–91.
25. Gómez C, Huerta FF, Yus M. DTBB-catalysed lithiation of chlorinated benzylic chlorides, alcohols, thiols or amines. Tetrahedron 1998;54:1853–66.
26. Shelanski ML, Gaskin F, Cantor CR. Microtubule assembly in the absence of added nucleotides. Proc Natl Acad Sci U S A 1973;70:765–8.
27. Weber K, Wehland J, Herzog W. Griseofulvin interacts with microtubules both *in vivo* and *in vitro*. J Mol Biol 1976;102:817–29.
28. Wehland J, Herzog W, Weber K. Interaction of griseofulvin with microtubules, microtubule protein and tubulin. J Mol Biol 1977;111:329–42.
29. Cizmecioglu O, Arnold M, Bahtz R, Settele F, Ehret L, Haselmann-Weiss U , et al. Cep152 acts as a scaffold for recruitment of Plk4 and CPAP to the centrosome. J Cell Biol 2010;191:731–9.
30. Raab MS, Podar K, Breitkreutz I, Richardson PG, Anderson KC. Multiple myeloma. Lancet 2009;374:324–39.
31. Loo DS. Systemic antifungal agents: an update of established and new therapies. Adv Dermatol 2006;22:101–24.
32. Gull K, Trinci APJ. Griseofulvin inhibits fungal mitosis. Nature 1973;244:292–4.
33. Grisham LM, Wilson L, Bensch KG. Antimitotic action of griseofulvin does not involve disruption of microtubules. Nature 1973;244:294–6.
34. Ho YS, Duh JS, Jeng JH, Wang YJ, Liang YC, Lin CH, et al. Griseofulvin potentiates antitumorigenesis effects of nocodazole through induction of apoptosis and G_2/M cell cycle arrest in human colorectal cancer cells. Int J Cancer 2001;91:393–401.
35. Panda D, Rathinasamy K, Santra MK, Wilson L. Kinetic suppression of microtubule dynamic instability by griseofulvin: implications for its possible use in the treatment of cancer. Proc Natl Acad Sci U S A 2005;102:9878–83.
36. Rønnest MH, Raab MS, Anderhub S, Boesen S, Krämer A, Larsen TO, et al. Disparate SAR data of griseofulvin analogues for the dermatophytes Trichophyton mentagrophytes, T. rubrum, and MDA-MB-231 cancer cells. J Med Chem 2012;55:652–60.
37. Roobol A, Gull K, Pogson CI. Evidence that griseofulvin binds to a microtubule associated protein. FEBS Lett 1977;75:149–53.
38. Rathinasamy K, Jindal B, Asthana J, Singh P, Balaji PV, Panda D. Griseofulvin stabilizes microtubule dynamics, activates p53 and inhibits the proliferation of MCF-7 cells synergistically with vinblastine. BMC Cancer 2010;10:213.
39. Zhou J, Panda D, Landen JW, Wilson L, Joshi HC. Minor alteration of microtubule dynamics causes loss of tension across kinetochore pairs and activates the spindle checkpoint. J Biol Chem 2002;277:17200–8.
40. Rathinasamy K, Panda D. Suppression of microtubule dynamics by benomy decreases tension across kinetochore pairs and induces apoptosis in cancer cells. FEBS J 2006;273:4114–28.

Published OnlineFirst August 31, 2012; DOI: 10.1158/0008-5472.CAN-12-2026

Cancer Research
The Journal of Cancer Research (1916–1930) | The American Journal of Cancer (1931–1940)

AACR American Association for Cancer Research

GF-15, a Novel Inhibitor of Centrosomal Clustering, Suppresses Tumor Cell Growth *In Vitro* and *In Vivo*

Marc S. Raab, Iris Breitkreutz, Simon Anderhub, et al.

Cancer Res 2012;72:5374-5385. Published OnlineFirst August 31, 2012.